PHYSICAL REVIEW B VOLUME 27, NUMBER 7 1 APRIL 1983

Magnetic and magneto-optical properties of bismuth-substituted gadolinium iron garnet films

P. Hansen, K. Witter, and W. Tolksdorf
Philips GmbH Forschungslaboratorium Hamburg, D-2000 Hamburg 54, Federal Republic of Germany
(Received 3 August 1982)

The saturation magnetization M_s, the uniaxial anisotropy K_u, the optical absorption α, the Faraday rotation θ_F, and the Faraday ellipticity ψ_F of epitaxial garnet films of composition $Gd_{3-x}Bi_xFe_5O_{12}$ have been investigated for $x \leq 1.43$. The temperature dependence of M_s and θ_F have been measured in the range $4.2\ \mathrm{K} \leq T \leq T_C$. The compensation temperature decreases and the Curie temperature increases linearly with the Bi content in accordance with data reported for bismuth-substituted yttrium iron garnets. The contribution of the bismuth to the rotation $\Delta\theta_F/x$ at $\lambda = 633$ nm was found to be $-23\,800\ \mathrm{deg\,cm^{-1}}$ and $-20\,600\ \mathrm{deg\,cm^{-1}}$ at $T = 4.2$ and 295 K, respectively. θ_F has been described in terms of the sublattice magnetizations inferred from the fit of the molecular-field theory to the saturation magnetization. The extracted magneto-optical coefficients exhibit a nonlinear variation with x for both octahedral and tetrahedral sites. The growth-induced anisotropy shows a linear dependence on x and reaches a value of $1.74 \times 10^4\ \mathrm{J\,m^{-3}}$ at $x = 1.43$. The optical absorption was measured for wavelengths ranging between 500 and 800 nm.

I. INTRODUCTION

Bismuth-substituted iron garnets have received much attention because of their high magneto-optical effects which made these materials very attractive for various fundamental investigations as well as for device applications such as displays,[1–3] printers,[4] gyrolasers,[5] or optical components.[6] In a recent paper we have reported the magneto-optical properties of gallium-substituted gadolinium-bismuth iron garnets[7] which are of particular interest for optical printing devices.[4] In this work we present results of the $Gd_{3-x}Bi_xFe_5O_{12}$ system to complete the picture of the influence of the bismuth on the temperature, concentration, and wavelength dependence of the Faraday rotation, the Faraday ellipticity, and the optical absorption. Furthermore, we discuss some additional aspects such as the maximum attainable rotations, the stress- and growth-induced anisotropies, and the influence of the bismuth on the superexchange interaction. The experimental results are presented in Sec. II and are interpreted and discussed in Sec. III. In particular, the temperature dependence of the Faraday rotation is described in terms of the sublattice magnetizations inferred from the fit of the molecular-field theory to the measured saturation magnetization. The magneto-optical coefficients have been determined as a function of the bismuth content.

II. EXPERIMENTAL RESULTS

A. Garnet material characterization

The garnet films of composition $Gd_{3-x-u}Bi_xPb_uFe_{5-v}Pt_vO_{12}$ were grown by liquid-phase epitaxy (LPE) onto (111)-oriented Ca-, Mg-, and Zr-substituted gadolinium and neodymium gallium garnet substrates. The lattice constants are $a_s = 1.24770$, 1.24935, and 1.25079 nm, respectively.[8] The films were grown from $PbO\text{-}Bi_2O_3\text{-}B_2O_3$–based fluxes.[9] Two melts were used, differing by the gadolinium content, which causes different growth rates. The bismuth content of the films was controlled by supercooling. The film thickness ranged between 2.5 and 21 μm. The cation compositions of the films were measured by electron-probe microanalysis.[10] The results for selected film compositions used for measurements of the temperature dependence are compiled in Table I together with the supercoolings ΔT_s. Sample 1 was grown from a bismuth-free $PbO\text{-}B_2O_3$–based flux at a low supercooling. The lead and platinum enter the crystal as impurities and are assumed to occupy essentially dodecahedral and octahedral sites, respectively. This is confirmed by lattice-misfit measurements and the magnetic data.

Nearly all films are exposed to a compressive stress. The perpendicular lattice misfit

 ©1983 The American Physical Society

TABLE I. Supercodings ΔT_s and chemical analysis data of epitaxial garnet films of composition $Gd_{3-x-u}Bi_xPb_uFe_{5-v}Pt_vO_{12}$.

Sample No.	ΔT_s (K)	x	u	v
1	5	0	0.010	0.010
2[a]	11	0.41	0.038	0.051
3	27	0.55	0.033	0.031
4	51	0.76	0.044	0.038
5	72	0.94	0.056	0.043
6	109	1.25	0.079	0.053
7	128	1.43	0.099	0.051
Error	±1	±0.03	±0.01	±0.005

[a]This sample was grown from a melt containing 15 at. % less gadolinium than the melt used for the growth of the other films.

$\Delta a^{\perp}=a_s-a_f^{\perp}$ varies in the range $-0.007 \leq \Delta a^{\perp} \leq 0.0005$ nm, where $a_f^{\perp}$ denotes the lattice constant perpendicular to the film normal. From these data and the lattice constants of the substrates the strain-free lattice constants of the films can be determined.[11] The results are shown in Fig. 1 (open circles). The solid circles represent data from polycrystalline materials.[12] The solid and dashed lines (films and bulk crystals, respectively) were calculated from the ionic radii.[13] The steeper slope for the films has solely to be attributed to the higher impurity content as compared to the bulk crystals. From these data the maximum bismuth content which can be achieved for these compositions can be estimated. For bulk iron garnets the maximum attainable lattice constant a_m(bulk) is 1.2540 nm (dashed-dotted line in Fig. 1).[14] For epitaxial films a higher maximum lattice constant a_m(film) can be realized where a_m(film) was estimated by

$$a_m(\text{film})=a_m(\text{bulk}) +[(1-\mu)/(1+\mu)]\Delta a^{\perp}=1.2580$$

in units of nm (dotted line). The maximum substitutional level x_m for bismuth in gadolinium iron garnet films thus is expected to be 1.7. The maximum value of the strain-free lattice constant calculated from the mismatch which has been achieved is 1.255 97 nm. Higher lattice constants are possible but the required substrates were not available. Additional aluminum substitutions increase this limit as shown by the solid lines calculated for a corresponding impurity content. For comparison experimental[12,14–20] and calculated lattice constants for the bismuth- and aluminum-substituted yttrium iron garnet system are shown yielding higher maximum values for x_m. Further, it can be concluded from the data presented in Fig. 1 that significantly higher bismuth substitutions are attainable than those reported for polycrystalline materials.[21]

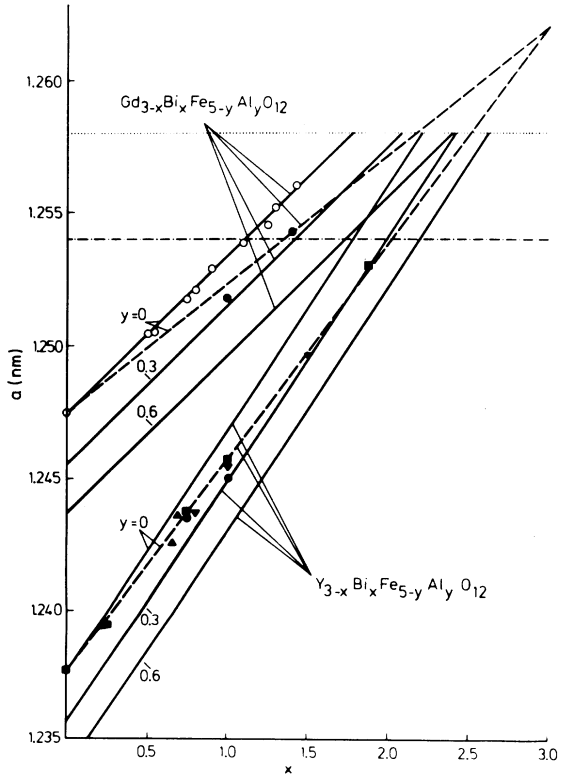

FIG. 1. Lattice constants vs bismuth content for gadolinium-bismuth and yttrium-bismuth iron-aluminium garnets. Open circles refer to the investigated garnet films and solid symbols are literature data (Refs. 12 and 14–20). Dashed and solid lines were calculated from the ionic radii (see text).

B. Magnetic properties

The saturation magnetization was measured with a vibrating-sample magnetometer in fields up to

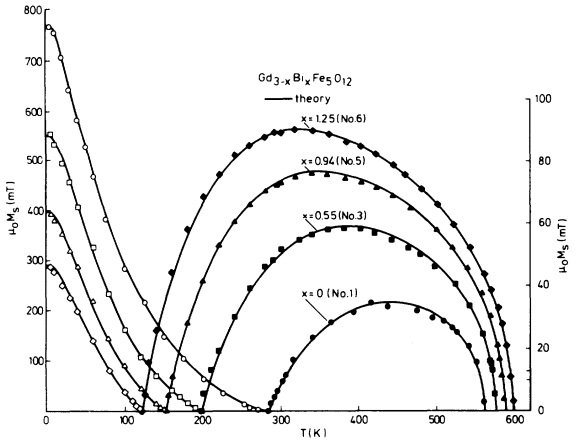

FIG. 2. Saturation magnetization vs temperature for different bismuth contents. Theoretical curves were calculated from the molecular-field theory. The data for $T < T_{comp}$ (open symbols) apply to the left-hand scale and those for $T > T_{comp}$ (solid symbols) to the right-hand scale.

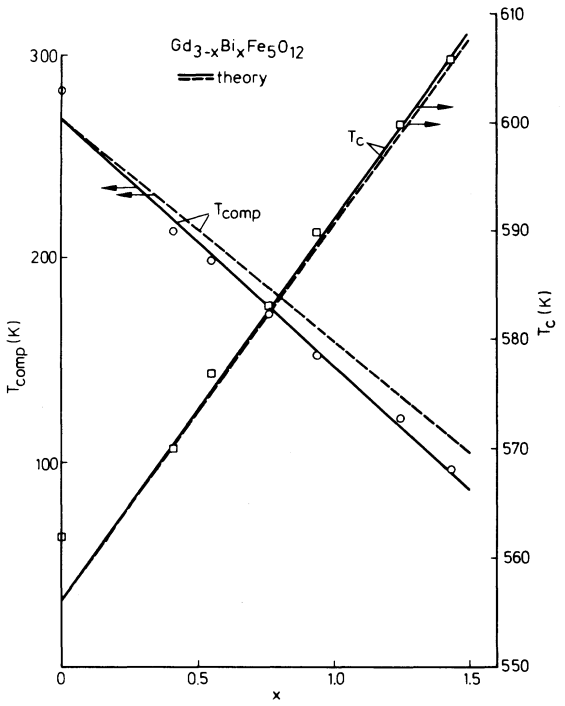

FIG. 3. Compensation temperature T_{comp} and Curie temperature T_C vs bismuth content. Solid and dashed lines were calculated from the molecular-field theory (see text).

1.6×10^6 A/m. The M_s data were obtained from an extrapolation to zero field. The temperature dependence of M_s for some compositions is shown in Fig. 2. The M_s value at $T=0$ K decreases linearly with increasing bismuth content owing to the dilution of the gadolinium sublattice. Furthermore, the bismuth raises the Curie temperature and reduces the compensation temperature substantially as shown in Fig. 3. This behavior must be attributed to the influence of the Bi ions on the superexchange interaction as it was reported for Bi-substituted yttrium iron garnets.[14–16] The T_{comp} values have been determined from the Faraday rotation exhibiting a sign change at T_{comp} at fixed direction of the external field. The solid and dashed lines represent the molecular-field theory and will be discussed in Sec. III. The magnetization data are summarized in Table II.

Bismuth-substituted iron garnets are characterized by a large uniaxial anisotropy aligning the magnetization parallel to the film normal. The measurement of the anisotropy was performed at $T=295$ K with a torque magnetometer. The uniaxial anisotropy constant K_u was evaluated from the torque $L(\alpha)$ using a plot of $L(\alpha)/H^2$ vs $L(\alpha)$, where α represents the angle between the film normal and the direction of the applied field H.[22] The presented data were extracted from the results obtained for $\alpha=45°$. For the measured samples the cubic anisotropy was negligible. K_u composes of a stress-induced and a growth-induced part expressed by the anisotropy constants K_u^λ and K_u^g, respectively,

$$K_u = K_u^\lambda + K_u^g ,$$
$$K_u^\lambda = -\frac{3}{2}\frac{\Delta a^\perp}{a}\frac{E}{1+\mu}\lambda_{111} . \quad (1)$$

TABLE II. Measured magnetic and magneto-optical (at $\lambda=633$ nm) data of the investigated garnet films.

Sample No.	x	$\mu_0 M_s$ (mT) $T=4.2$ K	$\mu_0 M_s$ (mT) $T=295$ K	T_{comp} (K)	T_C (K)	θ_F (deg cm^{-1}) $T=4.2$ K	θ_F (deg cm^{-1}) $T=295$ K
1	0	771	7	283	562	200	345
2	0.41	575	40	213	570	−9 560	−7 670
3	0.55	547	49	198	577	−13 600	−11 360
4	0.76	442	60	172	584	−17 670	−15 050
5	0.94	400	73	153	590	−23 120	−19 420
6	1.25	292	89	121	599	−31 340	−26 500
7	1.43	230	105	97	606	−33 200	−28 500

K_u^λ can be calculated from the relative perpendicular lattice mismatch $\Delta a^\perp/a$, the Young modulus E, the Poisson constant μ, and the magnetostriction constant λ_{111}. With the use of the values $\mu=0.31$ and $E=1.95\times10^{11}$ J m^{-3} which apply for $Gd_3Fe_5O_{12}$, λ_{111} can be derived from a plot of K_u vs $\Delta a^\perp/a$ at constant bismuth content yielding $\lambda_{111}=-3.6\times10^{-6}$ for $x=0.94$. This value can be compared with results from ferromagnetic resonance measurements which we have performed at 9.2 GHz on bulk crystals[23] of composition $Y_{3-x}Bi_xFe_5O_{12}$ yielding a contribution $\Delta\lambda_{111}/x=-0.7\times10^{-6}$ at $T=295$ K. Since the bismuth behaves similarly in gadolinium and yttrium iron garnets we expect λ_{111} to vary as

$$\lambda_{111}=-(2.9+0.7x)\times10^{-6}, \quad (2)$$

where the value of λ_{111} for $x=0$ was taken from Ref. 24. The magnetostriction constant obtained from Eq. (2) for $x=0.94$ agrees well with the value extracted before. On the basis of this good agreement we used Eq. (2) and the measured $\Delta a^\perp/a$ data to calculate K_u^λ as a function of the bismuth content. From the measured K_u values and these K_u^λ values K_u^g can be determined and the result is presented in Fig. 4. Whether the linear relationship obtained for high x is also valid for low x cannot be decided on the basis of the available data. For substituted gadolinium iron garnets exhibiting a compensation temperature near ambient temperature, the demagnetization energy is relatively small and thus it is evident from Fig. 4 that only a low Bi concentration

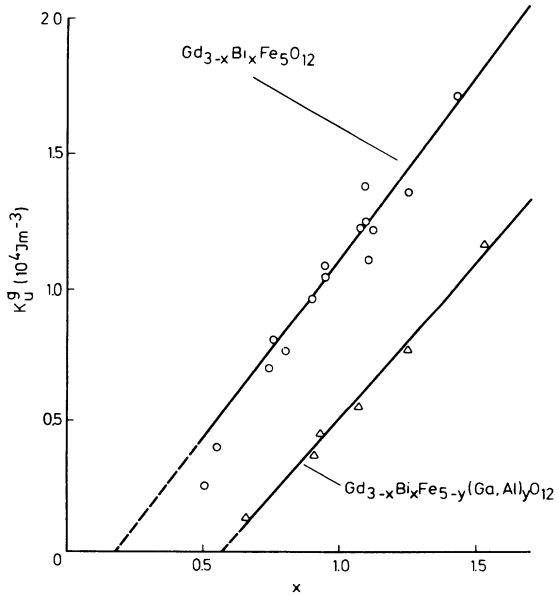

FIG. 4. Growth-induced uniaxial anisotropy constant vs bismuth content at $T=295$ K.

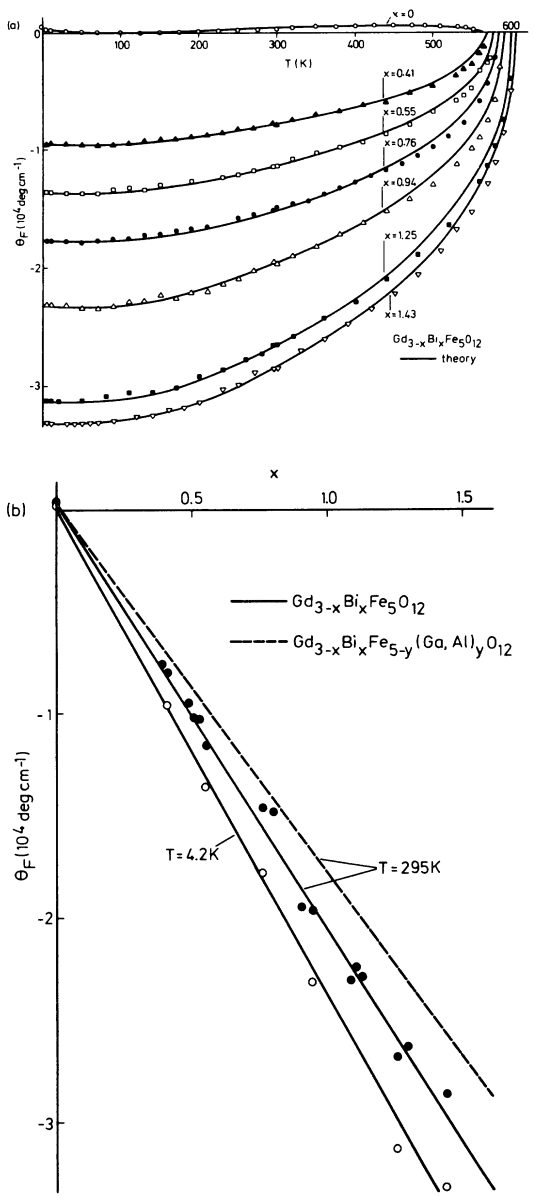

FIG. 5. Faraday rotation at $\lambda=633$ nm: (a) vs temperature for different bismuth contents, and (b) vs bismuth concentration. Theoretical curves in (a) were calculated from Eq. (4) (see text).

is necessary to obtain a positive uniaxial anisotropy provided K_u^λ is small. This results in a magnetization oriented perpendicular to the film surface as is required for certain device applications. The magnitude of K_u, however, strongly depends on the growth conditions as demonstrated by the K_u^g data for $Gd_{3-x}Bi_xFe_{5-y}(Ga,Al)_yO_{12}$ with $y\approx0.5$ which were grown at lower supercoolings. The K_u^g values reported for other bismuth-containing mixed rare-earth garnets are higher[25] since the rare-earth pairs also contribute to K_u^g.

C. Magneto-optical properties

The Faraday rotation and ellipticity have been measured with two different optical hysteresigraphs which were set up for temperature-dependent investigations at $\lambda=633$ nm in fields up to 1.3×10^6 A/m and for room-temperature measurements at $\lambda=546$ nm at lower fields.[26] The data were obtained from the recorded hysteresis loops by extrapolation to zero field. The temperature dependence of θ_F is shown in Fig. 5(a) for different bismuth contents at $\lambda=633$ nm. The sign change of θ_F occurring at T_{comp} has been omitted and the given rotations apply to a fixed direction of the sublattice magnetizations. The θ_F values appear to be slightly higher than those reported for polycrystalline garnets of corresponding composition.[12] The contribution $\Delta\theta_F$ of the lead impurities of concentration u to the rotation ($\Delta\theta_F/u\approx-7700$ deg cm^{-1}) is less than 3% of the total rotation.[7,27] The solid lines represent the θ_F dependences calculated from the sublattice magnetizations and will be discussed in Sec. III. The concentration dependence of θ_F at $\lambda=633$ nm is displayed in Fig. 5(b) yielding for $\Delta\theta_F/x$ $-23\,800$ deg cm^{-1} and $-20\,600$ deg cm^{-1} at $T=4.2$ and 295 K, respectively. For comparison the rotation for $Gd_{3-x}Bi_xFe_{5-y}(Ga,Al)_yO_{12}$ is given for $y\approx0.3$

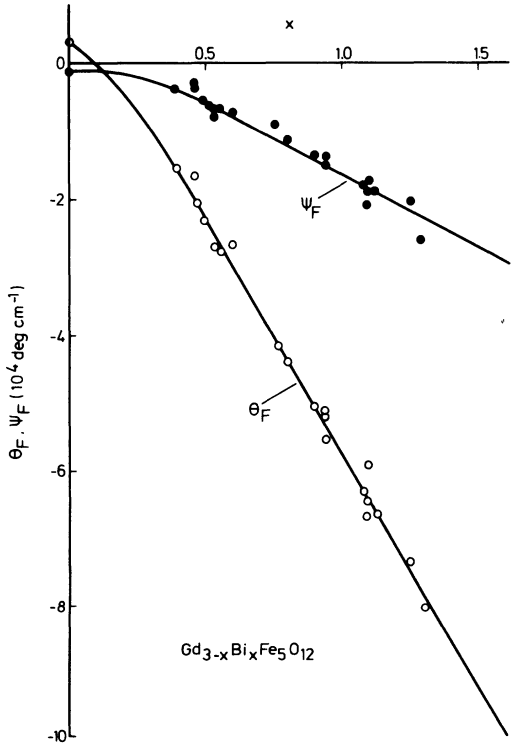

Fig. 6. Faraday rotation and Faraday ellipticity at $\lambda=546$ vs bismuth content at $T=295$ K.

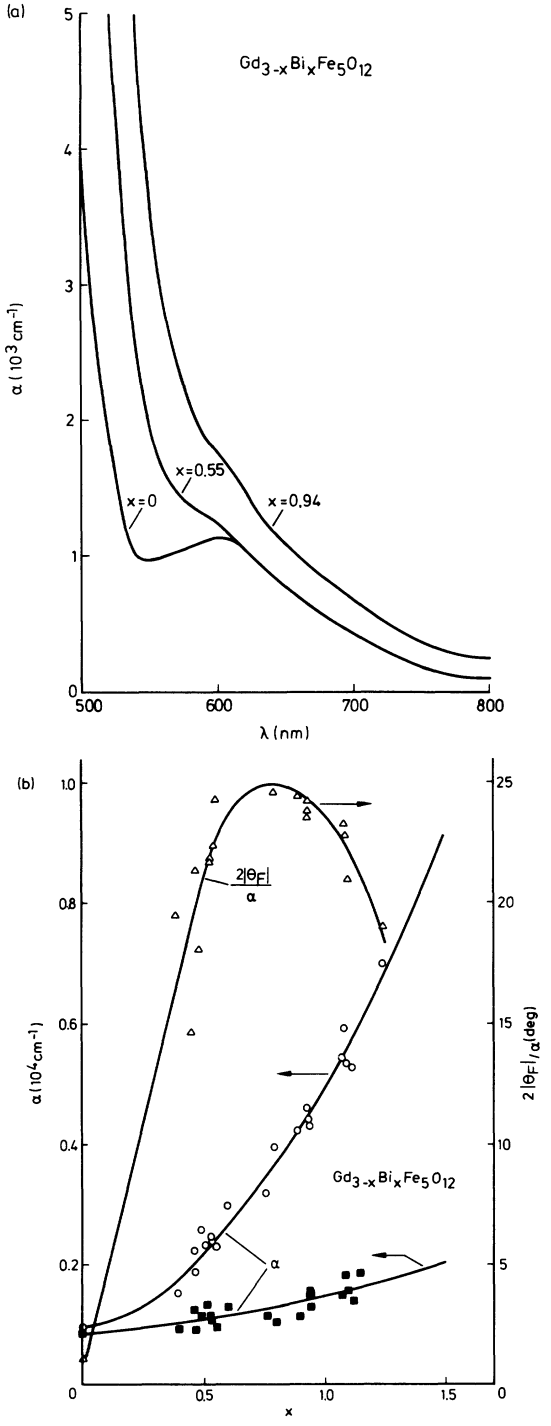

FIG. 7. (a) Optical absorption vs wavelength at $T=295$ K, and (b) optical absorption and figure of merit at $\lambda=564$ (open symbols) and 633 nm (closed squares).

(dashed line)[7] indicating the reduction of θ_F caused by diamagnetic tetrahedral substitution.[7,12] At shorter wavelengths the rotation strongly increases. In Fig. 6 the concentration dependence of θ_F is

displayed for $\lambda=546$ nm and $\Delta\theta_F/x$ is found to be roughly 3 times that at $\lambda=633$ nm. The data for the rotation at $T=4.2$ and 295 K are summarized in Table II for selected samples. The angle ψ_F corresponding to the Faraday ellipticity $\epsilon_F=\tanh(\psi_F L)$ is also significantly increased in the short-wavelength range as shown in Fig. 6 while at $\lambda=633$ nm and for higher wavelengths ψ_F approximately is not affected by bismuth and thus corresponds to that of pure $Gd_3Fe_5O_{12}$. L denotes the film thickness. The scatter of the ψ_F data is caused by the varying lead content since the lead contribution $\Delta\psi_F/u$ is roughly twice the bismuth contribution.[26] The data plotted in Fig. 6 indicate a deviation of ψ_F from linearity at low x values.

The optical absorption is shown in Fig. 7(a). The shift of the strong transitions of the band edge must be attributed to the bismuth while the increase for longer wavelengths essentially is caused by the lead when $x \gtrsim 0.5$ where $u > v$.[26] The concentration dependence of α is displayed in Fig. 7(b) for $\lambda=633$ nm (closed symbols) and $\lambda=546$ nm (open symbols). The scatter in the data again originates from the varying lead content and is more pronounced at $\lambda=633$ nm. Since ψ_F corresponds to the circular diochrism $\Delta\alpha$, the influence of the lead on ψ_F and α is comparable. For $x \lesssim 0.5$, Pb^{2+} is compensated by Pt^{4+} and in this range ψ_F remains unchanged by the Pb content in contrast to $x > 0.5$ where $u > v$. The figure of merit $2\theta_F/\alpha$ at $\lambda=546$ nm exhibits a maximum at $x \approx 0.8$ in agreement with Bi-substituted samarium iron garnets.[29] For $\lambda=633$ nm, $2\theta_F/\alpha$ is slightly higher and almost constant in the range $0.9 < x < 1.5$. At wavelengths $\lambda > 900$ nm for $2\theta_F/\alpha$, a steep increase is observed.[19]

III. DISCUSSION

A. Magnetic properties

The saturation magnetization of ferromagnetic garnets can be well described in terms of the molecular-field theory.[7,29,30] To account for the linear dependence of T_{comp} and T_C with x the molecular-field constants N_{aa}, N_{dd}, and N_{ad} of pure $Gd_3Fe_5O_{12}$ (Ref. 29) must be modified according to the relations

$$\begin{aligned} &N_{aa}=-65.0,\quad N_{dd}=-30.4,\quad N_{cc}=0\,,\\ &N_{ad}=96.9(1+C_1x)\,,\\ &N_{ac}=-3.44(1-C_2x),\quad N_{dc}=6.02(1-C_2x)\,, \end{aligned} \tag{3}$$

where a, d, and c refer to the octahedral, tetrahedral, and dodecahedral sites, respectively. The constants are expressed in mole cm^{-3}. The solid lines in Fig. 2 have been calculated on the basis of the analysis data given in Table I and these molecular-field constants. With $C_1=0.035$ and $C_2=0.08$, a good fit of the experimental data is obtained. The same value for C_1 was found for the corresponding system which additionally contains gallium and/or aluminum.[7] The solid lines in Fig. 3 have been calculated for an average content of Pb and Pt impurities. The experimental data of sample 1 are not in agreement with the theoretical curves owing to its considerably lower impurity content. The shift of the Curie temperature $\Delta T_C/x$ was found to be about 36 K provided a T_C value with an average lead content (of samples 2—7) is used as a reference at $x=0$. This value is in good agreement with the shift $\Delta T_C/x=38$ K reported for polycrystalline $Y_{3-x}Bi_xFe_5O_{12}$ garnets.[14] The dashed lines in Fig. 3 correspond to the case $C_2=0$. This approximation has been used in Ref. 7.

These results reveal a pronounced increase of the superexchange interaction between the octahedral and tetrahedral iron ions while that between the gadolinium and iron ions in average is reduced owing to the bismuth dilution. Different models have been proposed to explain this increase of the superexchange interaction. The structural mechanism[14,15] argues that the change of the bond lengths and angles causes a more favorable interaction geometry resulting in a stronger interaction strength between the iron and oxygen ions. The electronic mechanism[28] suggests that the observed magnetic and in particular magneto-optical effects induced by the bismuth are primarily electronic in origin. Obviously not only the size is responsible for these effects since otherwise, e.g., lanthanum also is expected to induce similar changes of the magnetic properties which have not been observed.[14] The lead ion also is a candidate and indeed shows magneto-optical effects[7,26] which are comparable with those of the bismuth. Unfortunately this ion tends to enter the crystal in the divalent and tetravalent state or in combination with other ions on tetrahedral or octahedral sites. Therefore, this ion also gives no clear answer whether the structural or the electronic model is the basic mechanism.

The large growth-induced anisotropies in bismuth-substituted iron garnet films indicate that presumably both the structural and electronic mechanism contribute to this property. The local deformations induced by the large Bi^{3+} ions define a "Bi complex" containing the surrounding Fe^{3+} ions which, therefore, experience an additional local axial crystalline field. These Bi complexes are assumed to be preferentially incorporated into the crystal along the growth direction yielding an ordering. This causes different numbers for the iron ions with different axes of distortions which are related to the

growth direction and are proportional to the bismuth content. In addition, the strength of the local distortion is affected by the ordering process. This configuration is expected to exhibit a growth-induced anisotropy in contrast to the case where the Bi complexes are randomly distributed. The magnitude of the uniaxial anisotropy is governed by the strength of the ordering process of the Bi complexes and the influence of the bismuth on the spin-orbit coupling via the electronic effect. In contrast to rare-earth iron garnets the growth-induced anisotropy cannot be reduced by annealing treatments indicating that a very stable ordering of these Bi complexes takes place. The single-ion model[31] predicts, for S-state ions, that the anisotropy depends on the numbers of ions with different axes of the local low-symmetry crystalline fields, the magnitude of these fields and that of the spin-orbit coupling where the first two quantities are expected to be influenced by the structural mechanism and the growth conditions while the spin-orbit coupling essentially is affected by the electronic mechanism.

Ferromagnetic resonance measurements reveal an increase of the cubic anisotropy constant and the magnetostriction constant (see Sec. II) with increasing bismuth content indicating the presence of a higher effective spin-orbit coupling as compared to bismuth-free garnets. Therefore, a large uniaxial anisotropy depending on the bismuth content and the growth conditions is expected. The influence of the latter is confirmed by the K_u^g data given in Fig. 4 for $Gd_{3-x}Bi_xFe_{5-y}(Ga,Al)_yO_{12}$ which were grown at significantly lower supercoolings as compared to the films with $y=0$. The shift in K_u^g was probably not caused by the Ga,Al content since the same result was obtained for the system $Y_{3-x}Bi_xFe_5O_{12}$ at corresponding supercoolings. Further, the concentration dependence of K_u^g shows that a certain level of Bi ions is necessary to be incorporated into the crystal to achieve an ordering of the Bi complexes. This level is increased for decreasing supercoolings. K_u^g turns out to be governed essentially by the supercooling ΔT_s and to increase linearly with ΔT_s provided the other growth parameters were kept constant. The influence of the melt composition and the saturation temperature on K_u^g appear to be of minor importance. However, it should be noticed that the magnitude of K_u^g in contrast to mixed rare-earth iron garnets[32] can also be affected by the growth rate, which depends, e.g., on the rotation of the sample during the LPE process.

B. Magneto-optical properties

The maximum Faraday rotations attainable in bismuth-substituted gadolinium iron garnets can be estimated from Figs. 1, 5, and 6. For $Gd_{3-x}Bi_xFe_5O_{12}$ the maximum bismuth content x_m is about 1.7. This limits the room-temperature Faraday rotation $|\theta_F|$ to values which will not exceed 3.5×10^4 and 10^5 deg cm^{-1} for $\lambda=633$ and 546 nm, respectively. If aluminum and/or gallium is added higher x_m values are possible. An aluminum content of $y=0.3$ shifts x_m from 1.7 to 2.1. However, a corresponding increase of θ_F cannot be achieved since a part of the gain in θ_F is lost by the corresponding iron dilution as indicated by the dashed line in Fig. 5(b). Since the optical absorption also decreases with y, the figure of merit of these compositions with additional diamagnetic tetrahedral substitution is slightly higher in the visible. The highest bismuth content of $x=1.62$ was obtained for the composition $Gd_{1.38}Bi_{1.62}Fe_{4.64}Ga_{0.20}Al_{0.16}O_{12}$ exhibiting a rotation of $-26\,000$ deg cm^{-1} at $\lambda=633$ nm. A further increase of the bismuth content could not be achieved since the required substrates with a high lattice constant were not available. In addition, other growth conditions are necessary to approach the limit given in Fig. 1.

The temperature dependence of the Faraday rotation can be expressed in terms of the sublattice magnetizations[33]

$$\theta_F=AM_a(T)+DM_d(T)+CM_c(T)\ , \tag{4}$$

where A, D, and C are the magneto-optical coefficients for octahedral, tetrahedral, and dodecahedral

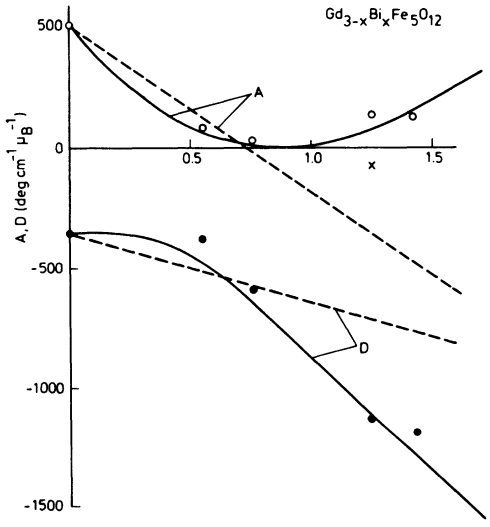

FIG. 8. Magneto-optical coefficients at $\lambda=633$ nm vs bismuth content. Dashed lines refer to $Gd_{3-x}Bi_xFe_{5-y}Ga_yO_{12}$ with $x\approx0.3$ (Ref. 7).

sites, respectively. These coefficients depend on wavelength and are determined by the electric and magnetic dipole transitions. θ_F can be calculated from the sublattice magnetizations. These are deduced from the fit of the molecular-field theory to the measured saturation magnetization. The magneto-optical coefficients were determined from the adjustment of θ_F to the measured data at two temperatures. For the dodecahedral coefficient the value for pure $Gd_3Fe_5O_{12}$ of $C=25$ deg cm$^{-1}\mu_B^{-1}$ was used neglecting its temperature dependence.[7] The temperature dependence of θ_F calculated for temperature-independent coefficients for $\lambda=633$ nm is shown by the solid lines in Fig. 5(a). Small deviations from the experimental data occur in the high-temperature range which can be removed if either the coefficients are assumed to depend on temperature or if higher order terms in Eq. (4) are taken into account.[34] The extracted magneto-optical coefficients are displayed in Fig. 8. Both the octahedral and the tetrahedral coefficients exhibit a nonlinear variation with the bismuth content. For comparison the results for gadolinium-bismuth iron-gallium garnets are shown[7] (dashed lines) indicating the significant influence of tetrahedral substitutions on these coefficients.

IV. CONCLUSIONS

The incorporation of bismuth into the crystals of gadolinium iron garnets strongly affects the superexchange interaction causing an increase of the Curie temperature and a decrease of the compensation temperature in accordance with results reported in literature for Bi-substituted yttrium iron garnets. The local deformations induced by the large ionic radius of the Bi ions and an ordering process along the growth direction leads to large uniaxial anisotropies for epitaxially grown films. The stress-induced anisotropy decreases ($\Delta a^{\perp}/a$ and λ_{111} decrease) and the growth-induced anisotropy increases with the bismuth content depending on the supercooling. The magnitude of the growth-induced anisotropy, in addition, depends primarily on the supercooling and the rate of rotation and less on the other growth parameters. It is almost not changed by annealing treatments.

The maximum magneto-optical effects attainable for these materials can be estimated from the maximum bismuth content. The magnitude of the Faraday rotation $|\theta_F|$ will not exceed values of 3.5×10^4 and 10^5 deg cm^{-1} for $\lambda=633$ and 546 nm, respectively. For $Y_{3-x}Bi_xFe_5O_{12}$, $|\theta_F|$ is limited to values lower than 4.5×10^4 deg cm^{-1} at $\lambda=633$ nm. The extracted magneto-optical coefficients reveal a nonlinear dependence on x.

ACKNOWLEDGMENTS

The authors would like to thank I. Bartels and C. P. Klages for the growth and preparation of the garnet films, P. Willich for the chemical analysis, and J. Schuldt and M. Rosenkranz for technical assistance. Helpful discussions with H. Heitmann are gratefully acknowledged.

[1]D. E. Lacklison, G. B. Scott, D. A. Giles, J. A. Clarke, R. F. Pearson, and J. L. Page, IEEE Trans. Magn. 13, 973 (1977).
[2]B. Hill and K.-P. Schmidt, Philips J. Res. 33, 211 (1978).
[3]B. Hill and K.-P. Schmidt, SID J. 10, 80 (1979).
[4]B. Hill and K.-P. Schmidt, in Conference Proceedings of the Congress on Advances in *N*-Impact Printing Technologies, Venice, 1981 (in press).
[5]J. J. Krebs, W. G. Maisch, G. A. Prinz, and D. W. Forester, IEEE Trans. Magn. 16, 1179 (1980).
[6]G. B. Scott and D. E. Lacklison, IEEE Trans. Magn. 12, 292 (1976).
[7]P. Hansen, H. Heitmann, and K. Witter, Phys. Rev. B 23, 6085 (1981).
[8]D. Mateika, R. Laurien, and C. H. Rusche, J. Cryst. Growth 56, 677 (1982).
[9]C. P. Klages and W. Tolksdorf (unpublished). The relationship between the growth conditions and the compositions of these films are to be published separately.
[10]P. Willich, W. Tolksdorf, and D. Obertop, J. Crys. Growth 53, 483 (1981).
[11]W. Tolksdorf, in *Physics of Magnetic Garnets,* edited by A. Paoletti (North-Holland, New York, 1978), p. 521.
[12]H. Takeuchi, Jpn. J. Appl. Phys. 14, 1903 (1975).
[13]B. Strocka, P. Holst, and W. Tolksdorf, Philips J. Res. 33, 186 (1978).
[14]S. Geller, H. J. Williams, G. P. Espinosa, R. C. Sherwood, and M. A. Gilleo, Appl. Phys. Lett. 3, 21 (1963); S. Geller, in *Physics of Magnetic Garnets,* Ref. 11, p. 1.
[15]S. Geller and A. A. Colville, in *Magnetism and Magnetic Materials—1974 (San Francisco),* Proceedings of the 20th Annual Conference on Magnetism and Magnetic Materials, edited by C. D. Graham, G. H. Lauder, and J. J. Rhyne (AIP, New York, 1975).
[16]T. J. A. Popma, A. M. van Diepen, and P. F. Bongers, J. Phys. Chem. Solids 35, 201 (1974).
[17]S. Wittekoek and T. J. A. Popma, J. Appl. Phys. 44, 5560 (1973).
[18]H. Takeuchi, Jpn. J. Appl. Phys. 13, 2059 (1974).
[19]H. Takeuchi, S. Ito, I. Mikami, and S. Taniguchi, J. Appl. Phys. 44, 4789 (1973).
[20]J. L. Page, private communication.
[21]K. Shinagawa and S. Taniguchi, Jpn. J. Appl. Phys. 13, 1663 (1974).
[22]H. Miyajima, K. Sato, and T. Mizoguchi, J. Appl. Phys.

47, 4669 (1976).
[23]The crystals have been supplied by J. L. Page, Philips Research Laboratories, Redhill, England.
[24]A. E. Clark, J. J. Rhyne, and E. R. Callen, J. Appl. Phys. 39, 573 (1968).
[25]L. C. Luther, R. C. LeCraw, J. F. Dillon, Jr., and R. C. Wolfe, J. Appl. Phys. 53, 2478 (1982).
[26]P. Hansen, M. Rosenkranz, and K. Witter, Phys. Rev. B 25, 4396 (1982).
[27]P. Hansen, W. Tolksdorf, and K. Witter, IEEE Trans. Magn. 17, 3211 (1981).
[28]G. B. Scott, D. E. Lacklison, J. L. Page, and J. Hewett, Appl. Phys. 9, 71 (1976).
[29]G. F. Dionne, J. Appl. Phys. 47, 4220 (1976).
[30]P. Röschmann and P. Hansen, J. Appl. Phys. 52, 6257 (1981).
[31]P. Hansen, in *Physics of Magnetic Garnets,* Ref. 11, p. 56.
[32]T. Hibiya and H. Makino, Mater. Res. Bull. 16, 847 (1981).
[33]W. A. Crossley, R. W. Cooper, J. L. Page, and R. P. van Stapele, Phys. Rev. 181, 896 (1969).
[34]P. Hansen and K. Witter, Phys. Rev. B 27, 1498 (1983).